RSC Advances

ROYAL SOCIETY OF CHEMISTRY

www.rsc.org/advances

Design, synthesis and photophysical properties of 8-hydroxyquinoline-functionalized tripodal molecular switch as a highly selective sequential pH sensor in aqueous solution

Rifat Akbar[1], *Minati Baral*[2] *and B K Kanungo*[1]*

[1]Department of Chemistry, Sant Longowal Institute of Engineering & Technology, Longowal, Punjab–148106, India

[2]Department of Chemistry, National Institute of Technology Kurukshetra, Haryana–136119, India

b.kanungo@gmail.com

Abstract

The development and photophysical properties of biomimitic analogue of microbial siderophore from quinolobactin have been described. The impudent analogue, 5,5'-(2(((8-hydroxyquinolin-5-yl)methylamino)methyl)2-methylpropane-1,3-diyl)bis(azanediyl)-bis-(methylene)diquinolin-8-ol, (TAME5OX), has been synthesized by three bidentate 8–hydroxyquinoline (8HQ) groups, connected to 1,1,1–tris(aminomethyle) ethane framework, was selected for its potential applications in chemical and biological fields. A combination of absorption and emission spectrophotometry, potentiometry, electrospray mass spectrometry, nmr, ir and theoretical investigation were used to fully characterize TAME5OX. The intense fluorescence from TAME5OX get quenched intermittently under acidic and basic conditions due to the photoinduced intramolecular electron transfer (PET) from excited N–pyridyl to hydroxyl moiety of 8HQ units. This renders the ligand as OFF–ON–OFF type of pH-dependent fluorescent sensor. DFT was employed for optimization and evaluation of vibrational modes, excitation and emission properties of the protonated, neutral, deprotonated states of the analogue. Anomalous enhancement observed in the fluorescence spectra of the neutral form of sensor can be attributed to subtle structural differences from its cationic and anionic forms. Plausible explanations for low fluorescence of the acidic as well as basic form, were provided.

Keywords: biomimitic analogue; quinolobactin; microbial siderophore; fluorescence; DFT; OFF–ON–OFF sensor.

***Correspondence:** B. K. Kanungo, Department of Chemistry, Sant Longowal Institute of Engineering & Technology, Longowal-148106, Punjab, INDIA.

Email: b.kanungo@gmail.com; Ph. No. : +91-1672-253166 (O), +91-1672-253167 (R); FAX: +91-1672-280057.

1. Introduction

Out of seven potential quinolinols, only 8-hydroxyquinoline (8-HQ) can readily form a five-membered chelate complex with metal ions.[1] An important property that makes 8-HQ even more interesting as a chelator is the significant change in its fluorescence behaviour.[2] Therefore, 8-HQ has been used extensively to construct highly sensitive fluorescent chemosensors for sensing and imaging of metal ions of important biological and/or environmental significance,[3-6] and its chelates, in particular those with Al^{3+}, are major components for organic light-emitting diodes (OLEDs).[7] Due to their high thermal stability, excellent electron-transport properties, and unique luminescent properties,[8-9] many derivatives of 8-hydroxyquinoline (for example, substituted at 2, 3,or 7 position in tri or tetrapodal orchestration, and/or coordinated with different metal ions) (Figure 1) have also attracted considerable interest. The importance of metalloquinolates in analytical chemistry is also well known.[10] In addition, a large number of 8-hydroxyquinoline derivatives have been synthesized and shown to be bioactive. For example, it was reported that some 8-hydroxyquinoline derivatives possess antitumor and antimicrobial activities.[11]

It is known that the excited-state intramolecular proton transfer (ESIPT), from 8-OH to the quinolino-N atom, makes 8-HQ weakly fluorescent and metal binding to 8-HQ blocks the ESIPT channel, thereby restoring the fluorescence.[2,5] 8-HQ could hence be employed to build fluorescent chemosensors with increased fluorescence signal upon metal binding via

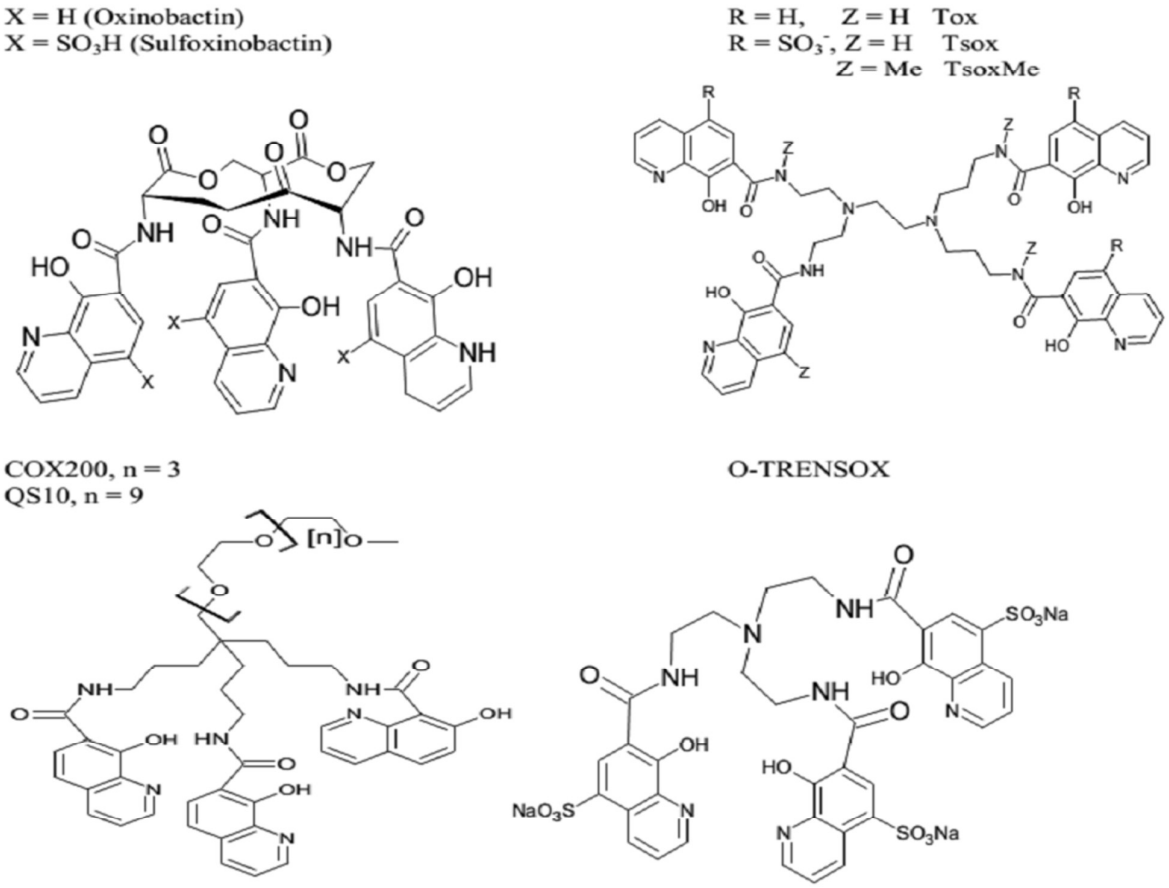

Figure 1. Structures of Oxinobactin, Sulfoxinobactin, Tsox, TsoxMe, COX2000 and O-TRENSOX.

ESIPT suppression. To enhance metal binding selectivity of 8-HQ, introduction of additional moieties (central unit and connecting groups) at the C-2, C-3 and/or C-7 positions, adjacent to the original binding sites in 8-HQ (Figure 1), has been extensively examined.[3-6] In the case where 8-HQ was substituted with methyleneamine at the C-2 or C-7 position, a photoinduced electron transfer (PET) process leading to fluorescence quenching was identified,[4] and metal binding resulting in PET suppression was also established, which mechanism is currently intensively employed in constructing fluorescent chemosensors for transition metal ions operating under fluorescence enhancement mode.[12] Moreover, due to unique pyridyl –N and –OH structural features of 8–HQ unit, these end groups under acidic and basic conditions are able to act as a weak acid and a weak base, respectively, associated with the equilibrium

between the protonated quinolinium $NH^{+}\sim$–OH form and deprotonated quinolinate $N\sim O^{-}$ form,[13] this moiety appears to be able to act as the pH indicator for both acidic and basic systems. However, despite the large number of investigations on the fluorescent sensors with the 8-HQ moiety as receptor for metal ions,[14] there still exists very less exploration on the tripodal fluorescent sensors with 8-HQ moiety as pH indicator to the best of our knowledge. For the intention of preparing versatile fluorescent sensors for the acidic and/or basic systems, novel fluorescent compounds concurrently possessing three efficient 8-HQ receptor units should be developed. It is noted, however, that these investigations hitherto reported are limited mainly to 8-HQ derivatives with substituents on the C-2, C-3 or C-7 position.[15-18] Derivation at C-5 position of the 8-HQ has not been explored in detail. A possible reason could be that due to the para position of pyridyl N and OH groups in this arrangement, not much room remains for encapsulation of metal ions in the central cavity of ligand which facilitate coordination with more strain. However, further exploration revealed that substitution at the C-2, C-3 and/or C-7 positions in the 8-HQ moiety mainly tunes the coordinating property of the pyridyl N group, while substitution at the C-5 positions induces change in the binding ability of the OH group.[13] A preliminary molecular modeling study with molecular mechanics also attests the fact. As a consequence, designing and preparing novel fluorescent sensor in which the central unit is attached at the C-5 position are of interest. In the present paper, the novel 8-hydroxyquinoline based tripodal chelator, namely 5,5'-(2-(((8-hydroxyquinolin-5-yl)methylamino)methyl)-2-methylpropane-1,3-diyl)bis(azanediyl bis(methylene)diquinolin-8-ol, (TAME5OX), (Scheme 1) was reported, in which design relies on a short tris(aminomethyl)ethane (TAME) backbone as an anchor symmetrically fitted with three individual 8–hydroxyquinoline (8HQ) moieties at the C–5 position. The spacer bears a secondary amine function, and its length has been chosen to achieve a tight orientation of binding units. In continuation to our work on acyclic tripodal

chelates with 8-hydroxyquinoline units,[19-20] in this present communication, the synthesis, characterization and the detailed photophysical investigation of the new ligand is described to explore the pH dependent fluorescent behaviour of chelator.

2. Experimental

2.1 Materials and Methods

All manipulations were carried out under an atmosphere of nitrogen using standard cannula technique. All reagents were purchased from Sigma–Aldrich at the highest commercial quality, Alfa Aesar or Acros Organics, and used without further purification unless otherwise stated. Solvents were distilled freshly, refluxed over appropriate drying agents following standard procedures and kept under argon atmosphere. Melting points were determined on melting point apparatus and are uncorrected. Reactions were monitored by thin layer chromatography (TLC), performed on silica gel G plates using hexane and ethyleacetate (7:3), chloroform and methanol (4:1) as eluents; developed TLC plates were visualized by iodine vapours. Elemental analysis (CHN) was performed on the elemental analyzer Euro Vector S.P.A–81328 (Euro EA). Infra–red spectra were recorded using an Agilent Technologies Cary 630 FTIR spectrometer equipped with a universal attenuated total reflection (ATR) sampler and samples were directly used for obtaining IR spectrum. ^{1}H and ^{13}C NMR spectra were recorded in DMSO–d_6 using a Joel 300 (MHz) ECX spectrometer. Chemical shifts are reported in δ values related to an internal reference of tetramethylsilane (TMS). Mass analysis was performed in a TOF MS ES+ instrument. For solubility reason the ligand was converted to its hydrochloride salt and potentiometric and spectrophotometric studies were carried out in water purified by a Millipore Milli–Q water purification system. Ionic strength was adjusted with 0.1M KCl. All the stock solutions were prepared by weighing appropriate amounts by using GR–202 electronic balance (precision 0.01 mg) in Millipore grade deionized water. The exact concentration of KOH (0.1 M) was determined

potentiometrically using 0.1 M solutions of succinic acid, potassium hydrogen phthalate (KHP) and oxalic acid as primary standards and then the exact strength of HCl (0.1N) was determined by same method using standardized KOH. All the solutions were prepared with Millipore grade deionized water immediately before use, which was deoxygenated and flushed continuously with Ar (U grade) to exclude CO_2 and O_2. All measurements were carried out at 25.0 ± 0.2°C maintained with the help of Julabo F–25 thermostat.

2.2 Synthesis of TAME5OX

The synthesis of ligand was carried out by chloromethylation of the oxine **2** followed by condensation with tripodal 1,1,1 tris (aminomethyl) ethane) **1c** as depicted in Scheme 1. The synthesis of 5-chloromethyl-8-hydroxyquinoline hydrochloride **2a** was carried out with higher yields by the reported procedure.[21] The synthesis of 1,1,1 Tris (aminomethyl)ethane (TAME) **1c** was carried out under multistep reactions by the reported procedure.[22] The detailes of procedure for synthesis of **1c** and **2a** are presented in supplementary material.

2.2.1 5,5'-(2-(((8-hydroxyquinolin-5-yl)methylamino)methyl)-2-methylpropane-1,3-diyl)bis(azanediyl)bis(methylene)diquinolin-8-ol (TAME5OX) (**3**).

To a suspension of **2a** (138.28 mg, 0.6mmol) was added 1,1,1 tris (aminomethyl) ethane **1c** (23.4 mg, 0.2 mmol) in an acetone–water mixture and K_2CO_3 (82.92 mg, 0.6 mmol) was used as an acid acceptor. The mixture was refluxed with stirring on magnetic stirrer for 3 hrs. The suspension gets dissolved upon reflux and the colour changed from yellow to brown with the progress of reaction. The resulting mixture which contained brownish green precipitate after cooling at room temperature, was poured into ice cold (50 mL) water and then filtered. The solid product was collected, washed several times with diethylether and dried in vaccuo to

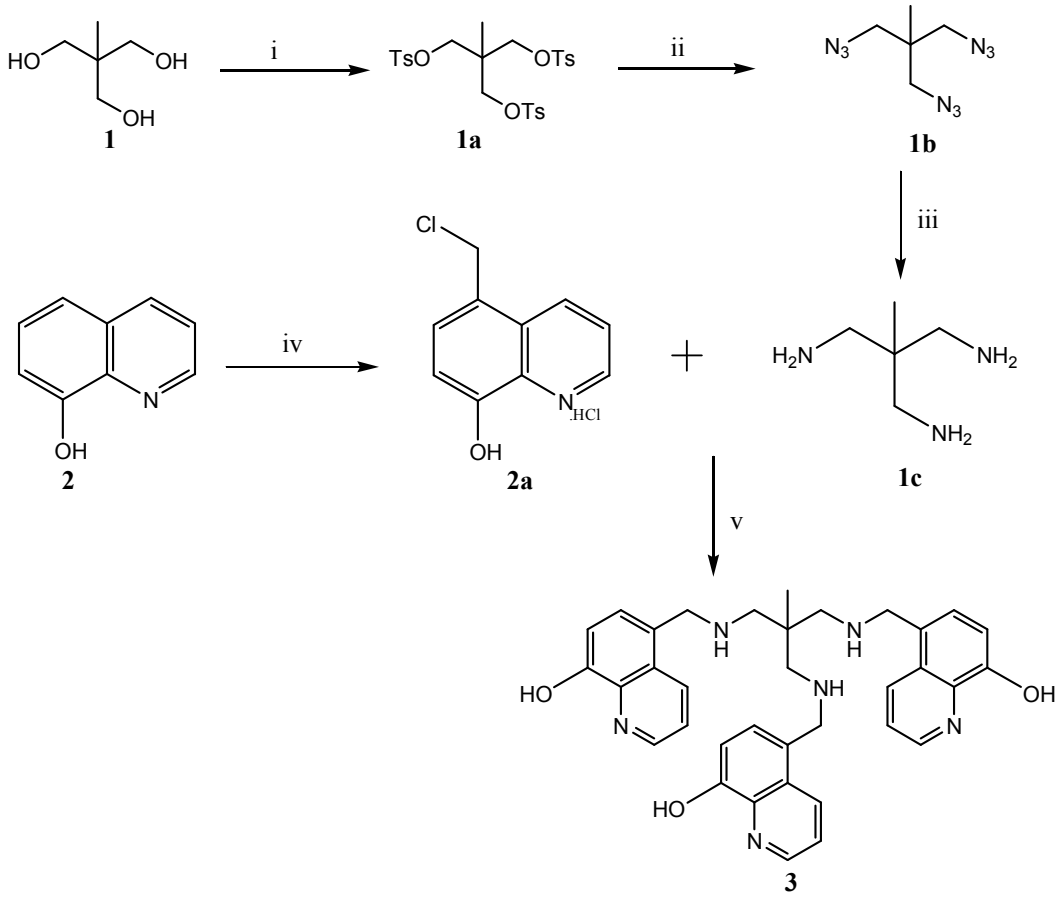

Scheme 1: Reagents and conditions: (i) NaOH:H_2O, TsCl, THF, 0°C, 6 hrs; (ii) NaN_3, DMSO, 137°C, 12 hrs, under N_2; (iii) $LiAlH_4$, dry THF, reflux, 18 hrs, under N_2; (iv) HCHO, 37% HCl, 50°C, 7 hrs, dry HCl gas;(v) K_2CO_3, acetone:water, reflux, 3 hrs.

afford TAME5OX 3 as a off white colour powder (0.085mg, 0.17mmol, 77%). m.p. 160°C; ^{1}HNMR (DMSO d_6, 25°C, TMS): δ = 1.18(s, 3H, CH_3); 2.05(s, 6H, CH_2); 2.4 (s, 6H, CH_2); 4.61 (s, 3H, NH); 8.42(d, $^3J_{H,H}$ = 6.8 Hz, 3H, Ar–H); 8.84(d, $^3J_{H,H}$ = 7.8 Hz, 3H, Ar–H); 6.91–6.94(t, $^3J_{H,H}$ = 7.6 Hz, 3H, Ar–H); 7.49-7.55(dd, $^3J_{H,H}$ = 8.0 Hz, 6H, Ar–H); 9.74(s, 1H, OH) ppm. ^{13}CNMR (DMSO d_6): δ = 37.01 (CH_3), 57.45 (CH_2), 62.66 (CH_2), 111.44, 117.88, 121.93, 127.57; 135.97, 138.34, 148.87, 152.51 (C=N), 153.58 (C–O). IR (ATR) ν(cm^{-1}) = 3470, 1594, 1454, 1396, 1239, 1172, 1080. Elemental analysis Calcd (%) for $C_{35}H_{36}N_6O_3$: 71.41 C; 6.16 H; 14.28 N; found: 71.66 C; 6.21 H; 14.35.N. MS (ES^+), m/Z (I,%) 598.2$[M+3]^+$(20).

2.3 Solution Thermodynamics: Potentiometric, Spectrophotometric and Fluorescence measurements

The pH meter, absorption and luminescence spectrophotometer used, experimental details, calibration of the electrode, titration procedures and quantum yield determination were used as described before.[19] Hydrochloride salt of ligand (5ml, 1×10^{-4}M) was titrated with standardized 0.095 M KOH for potentiometric titrations for the determination of protonation and formation constant, respectively. Spectrophotometric titrations of a 50mL solution of TAME5OX (5×10^{-5} M) in aqueous medium and acidified with approximately 5mL (0.1M) HCl, ionic strength maintained at 0.1 M with KCl were monitored as a function of pH over the range 1.6–10.8 by titrating with freshly prepared standardized (0.1M) NaOH solution. After each addition of NaOH and adjustment of pH, it was ensured that complete equilibrium was attained (ca. 5 minutes) before measurement of the pH and UV–visible absorption spectrum. The method adopted for the fluorescence titrations are similar to the spectrophotometric titrations. Fluorescence spectra were registered with excitation at 385 nm and all excitation and emission slit widths at 5.0 nm unless otherwise indicated.

2.4 Theoretical Calculations

All computations were carried out on a Pentium IV 6.0 GHz machine with a Linux operating system. Initial geometry optimization and conformational analysis of the TAME5OX and its protonated and deprotonated species were performed using the approach already described.[20] The PM6 optimized molecular structures were then used for DFT level calculations. All the calculations including geometry optimization, harmonic vibrational frequency analysis, NBO analysis and ground state electronic transitions were performed by employing the B3LYP (Becke three parameter Lee–Yang–Parr)[2] exchange–correlation functional with the all–electron 6–31G* basis set was used. All possible protonated and deprotonated states of ligand (TAME5OX) described experimentally [$(LH_9)^{+6}$, $(LH_8)^{+5}$, $(LH_7)^{+4}$, $(LH_6)^{+3}$, $(LH_5)^{+2}$,

$(LH_4)^{+1}$, (LH_3), $(LH_2)^{-1}$, $(LH)^{-2}$ and $(L)^{-3}$] were also optimized at DFT level. To each optimized molecule, the Hessian was calculated for the resultant stationary points and all were characterized as true minima (i.e., no imaginary frequencies). The cartesian (*x*, *y*, *z*) coordinates of minimized structures are reported as supplementary information (Table S1-S10). Dispersion corrected DFT calculations were carried out for all the molecules using B3LYP-D3 functional [23] with zero-damping. The theoretically obtained dispersion and dispersion corrected energies for these structures are reported as supplementary information (Table S11). ^{1}H and ^{13}C NMR chemical shifts were calculated from the optimized molecule, by the Guage–Including Atomic Orbital (GIAO). All relative chemical shifts (δ) are given with respect to the absolute shielding values (σ) obtained at the same computational level (δ = (σ_{ref}–σ). The calculated vibrational wavenumbers and chemical shifts were compared with the experimental data of TAME5OX. To obtain the electronic transition energies (which include some account of electron correlation) in ground state for various acid–base species of TAME5OX, Time–Dependent Density–Functional Theory (TD–DFT) with same functional and basis sets as for geometry optimizations, were used.

The excited states were computed at the TD–DFT level, the cam–B3LYP density functional[16] with the all electron Pople double–ζ basis set including one diffusion functions on heavier atoms 6–31G*. The low–lying excited–state structure (*S*1) was optimized using the cam–B3LYP. This functional makes use of the Coulomb attenuation method and has been specifically parameterized with electron excitation processes in mind. To obtain properties of the first excited state (S1) such as structure, free energy, absorption and emission energies, three excited states were always included in the calculations. Emission wavelengths were evaluated on the TD–DFT (cam–B3LYP) optimized structures of the excited state. All of the computational results have been performed using the *Gaussian 09* [23] being used for spectra convolution and molecular orbital plots.

3. Results and Discussion

3.1 Design, Synthesis and Characterization

For an effecient metal chelator for trivalent metal ions with high complexing ability requires a topology which has a pivotal basic skeleton with suitable spacer length with attachment position of the binding unit; it is essential that the three electron donating arms should arrange themself around the tripodal ligand to work cooperatively for uptake of the cation. Keeping the above fact in view, we tried to design a suitable molecular edifice (TAME5OX) containing tris (aminomethyl) ethane as a central unit, anchored on a quaternary carbon, and extended by three diverging arms bearing the oxine coordination sites, connected at the C–5 position of the 8–hydroxyquinoline than commonly used C-2, C-3, or C-7 positions[15-18]. The whole synthesis of the TAME5OX was performed through a multistep pathway by following the general plan as depicted in Scheme 1, leading to a more reliable procedure.

Commercially available (Sigma–Aldrich) 1,1,1–tris(hydroxymethyl)ethane, **1**, the synthetic precursor bearing a methyl group at the bridgehead carbon, was converted to its tritosylate **1a** by a nucleophilic substitution reaction with tosyl chloride in THF. Intermediate tritosylate **1a** was isolated in high yield as white crystalline solid which was further reacted with sodium azide in DMSO to afford the corresponding triazide **1b**. The crude azide was obtained as slightly yellow oil and was used immediately after work–up to avoid explosion risks (see caution in section 4). Subsequent reduction of the triazide with LiAlH gave the required triamine (1,1,1 tris amino methyethane) **1c** in good yield. Since the triamine is a malodorous air sensitive liquid, it was converted to its corresponding salt as stable white solid by passing dry HCl gas into it. Triamine has been prepared by reported procedure[24] with slight changes.

The derivatization of oxine starts from 8-hydroxyquinoline **2**, a very cheap precursor, which is easily transformed into a 5–chloromethyle derivative **2a** by chloromethylation of

8–hydroxyquinoline at 5–position[21] (Scheme 1). The chloromethylation step is best done with formaldehyde (40%) and HCl (37%).[25] It has been reported that the synthesis of the free base **2a** could be carried out by the reaction of its hydrochloride salt with sodium hydrogen carbonate($NaHCO_3$)[26]; however, **2a** is unstable and readily undergo hydrolysis to form hydroxymethyl quinolinol.[25] Hence, the hydrochloride salt of **2a** was directly used for coupling. The synthesis of the final product, novel tripodal ligand based on C_3 symmetrical carbon anchor (TAME5OX **3**), involve direct condensation of hydrochloride salts of **1c** and **2a**. The reaction was performed by a conventional method, refluxing in acetone water mixture (because of insolubility of hydrochloride salt of **1c** and **2a** in organic solvents) in presence of K_2CO_3 for 3 hrs, which led formation of the final product, TAME5OX, **3**. The compound was isolated as an air–stable brownish green colour solid, recrystalised from chloroform as pure compound with 96% yield and was characterized by CHN analysis, FTIR, ^{1}H, COZY and ^{13}C NMR and mass spectrometry.

3.1.1 Infrared spectra

Figure 2 shows comparison of experimental and theoretical IR spectra of the TAME5OX. The absorption peak at 3399 cm^{-1} of TAME5OX is ascribed to the –OH stretching of 8–hydroxyquinoline unit. The band observed at lower frequency than the normal position of free oxine, 3730–3520 cm^{-1}, is attributed to presence of intramolecular hydrogen bonding in the ligand, which can be also seen in ^{1}H NMR of TAME5OX. The appearance of bands at 2925 and 1469 cm^{-1} are due to N–H stretching and bending vibrations, respectively of $–CH_2–NH–CH_2–$ spacer, and no peak attributable to unreacted amine or chloromethylene group was present. The absorption peaks around 1599, 1556 and 1389 cm^{-1} are due to the aromatic carbon–carbon stretching vibrations due to 8–hydroxyquinoline nucleus.[25] The weak bands around 2112 and 1786 cm^{-1} may be due to asymmetric and symmetric stretching

vibrations of methylene groups (–CH_2–), and near 1300 cm^{-1} and 1320 cm^{-1} are due to asymmetric and symmetric stretching vibrations of the –CH_2–NH–CH_2–bridge.

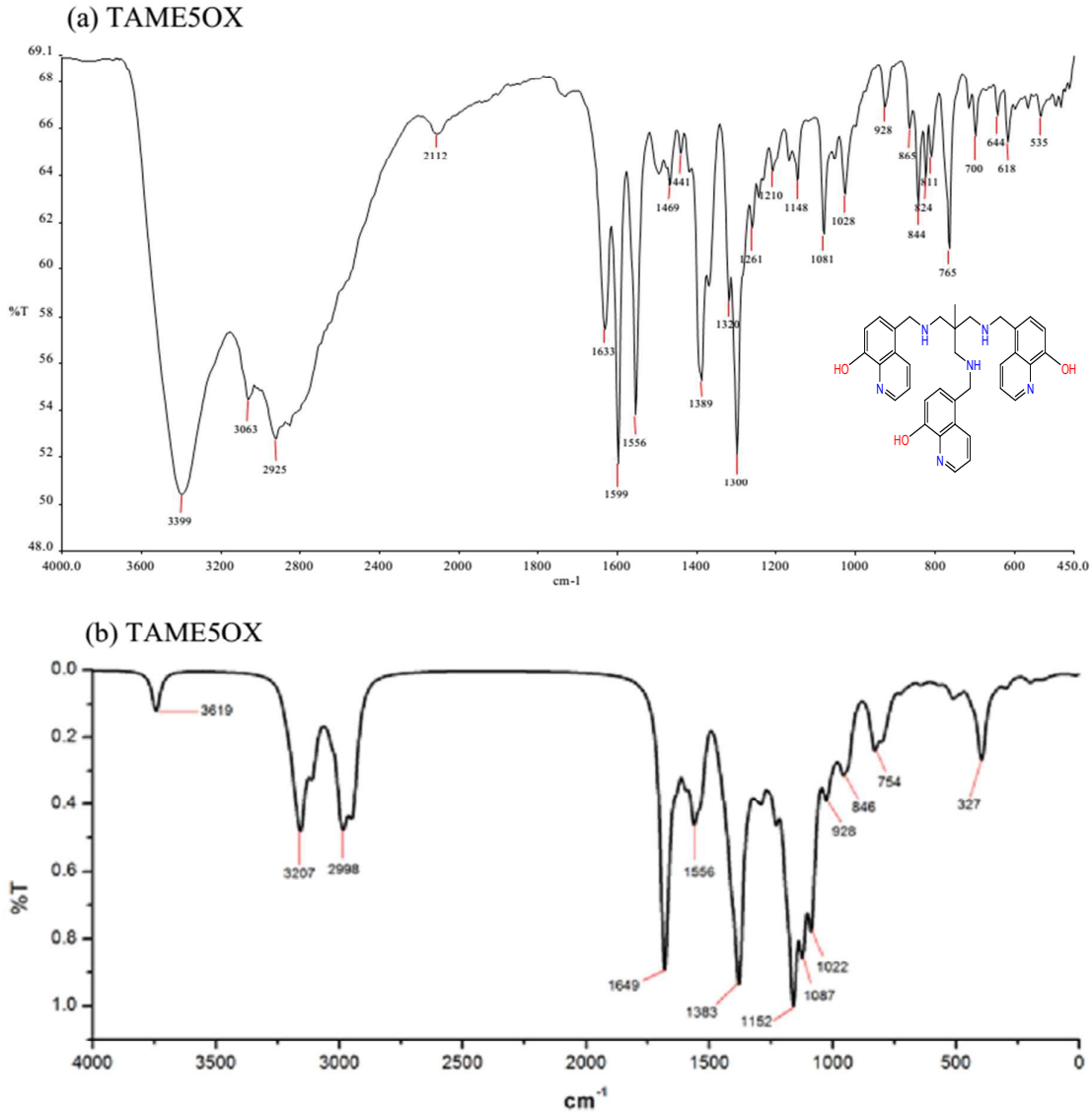

Figure 2: Infra–red (IR) spectrum of TAME5OX (a) experimental (KBr) (b) theoretical (calculated by B3LYP/6–31G*).

In order to confirm the assignments of IR frequencies, theoretical calculations were carried out by DFT method at B3LYP/6-31G* level. The calculated IR frequencies of the TAME5OX are shown in Figure 2. For comparison, the theoretical and experimental values are also given in table 1. The calculated vibrational frequencies are obtained at higher values

than experimental ones, but their trend are corroborate with the experimental data indicating that theoretical results can be implemented for the interpretation of experimental results. The differences in calculated and experimental spectra may be mainly due to, somewhat, to the fact that the experimental spectra were measured in the solid phase and the theoretical spectra were obtained in the gas phase. However, a linear correlation obtained between the theoretical and experimental data (Figure 3) gave an acceptable correlation.

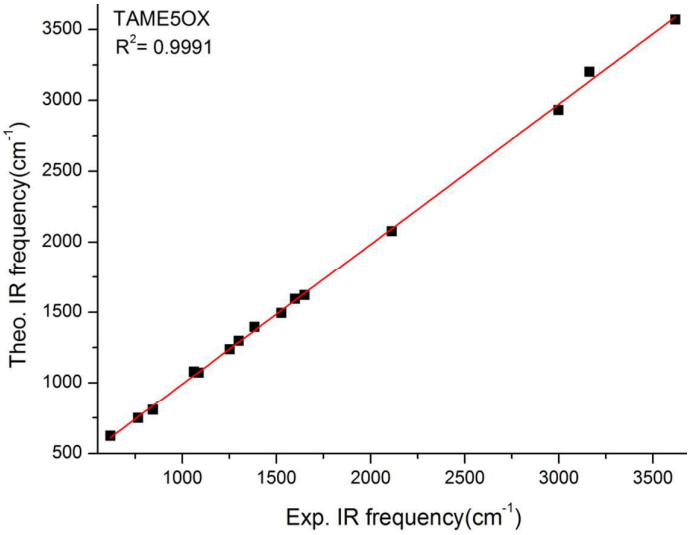

Figure 3: Correlation between the experimental and theoretical IR frequencies of TAME5OX

3.1.2 NMR Spectra

The ^{1}H NMR of TAME5OX presents set of signals given in section 2.3 with the assignments proposed on the basis of the numbering scheme are given in 'a' of Figure 4. On proton NMR spectra of the ligand, signals were observed characteristics to OH, CH, CH_2 and CH_3 protons. Signals due to CH of 8–hydroxyquinoline were observed in the aromatic region of the spectrum in the range of 8.87–6.9 ppm (inset of figure 4) which showed two doublets at 8.4 and 8.8 ppm, one double doublet at 7.5 and one triplet around 6.9 ppm. Singlets at 1.1, 2.0 and 2.4 ppm are assigned to the protons of one methyl (–CH_3) and two methylene (–CH_2)

groups: one attached to carbon of centre unit, and the other to 8–hydroxyquinoline unit, respectively. TAME5OX showed a signal at 4.61 ppm due to NH proton and board peak at

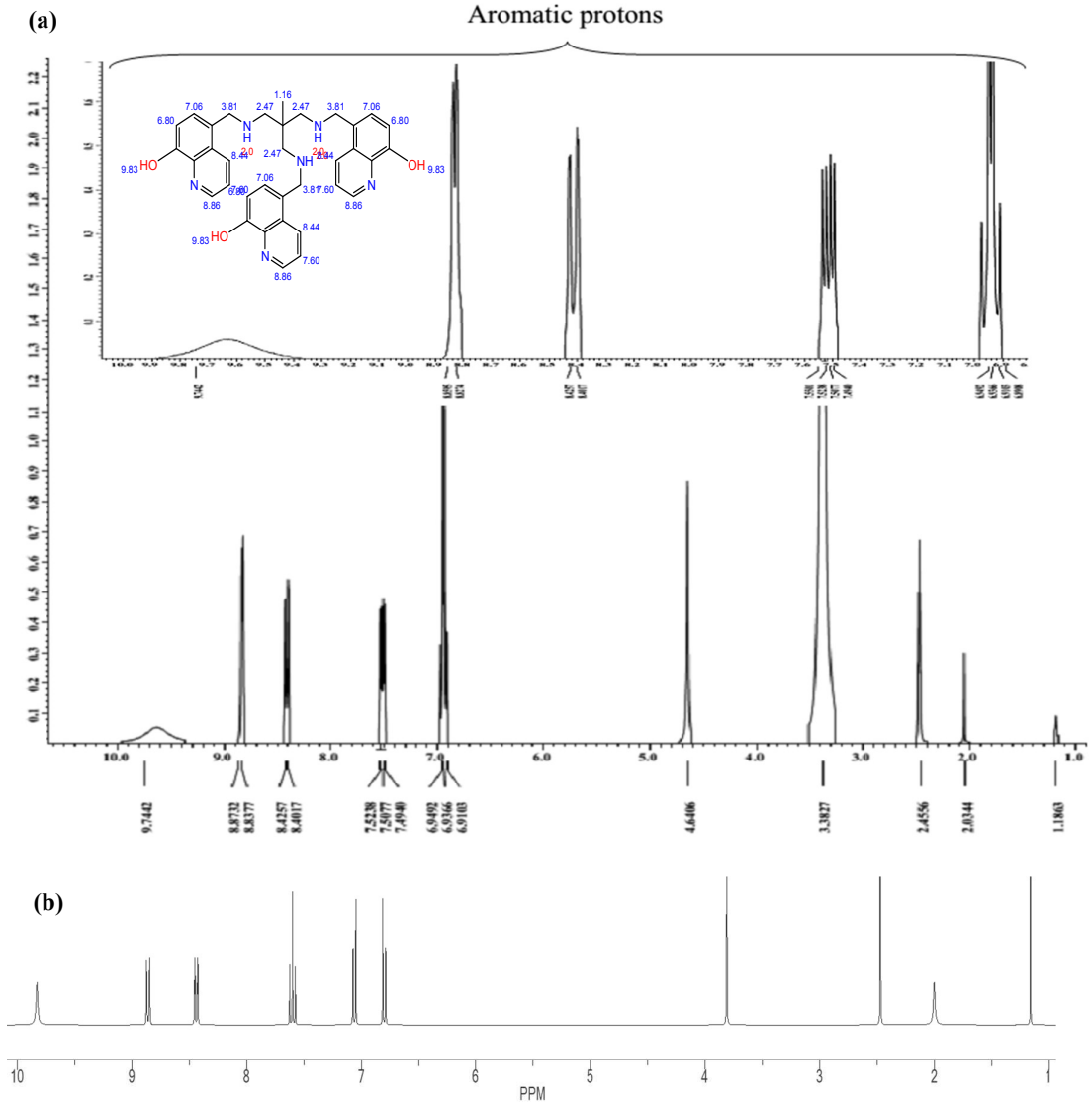

Figure 4: [1]HNMR spectrum of TAME5OX: (a) experimental (DMSO, 300 MHz), inset showing splitting of protons of aromatic part of ligand, and (b) calculated (applying DFT/B3LYP/6–31G* method).

9.74 ppm for hydroxyl proton of quinoline ring; this weak and broad band of hydroxyl protons observed were most probably resulted from intramolecular H–bonding of OH proton with N atom of quinoline unit.[27]

The ^{13}C NMR spectrum of TAME5OX, with the assignments proposed on the basis of the numbering scheme, is given in Figure 5. The ligand showed bands at 34, 56 and 61 ppm due to the CH_3 and CH_2–NH–CH_2 carbons, respectively. Signals at 148, 139, 135, 127, 126, 122, 120 and 110 ppm attributed to the CH groups belong to aromatic oxine unit, whereas the peak at 153 ppm corresponds to carbon attached to –OH present in the oxine unit.

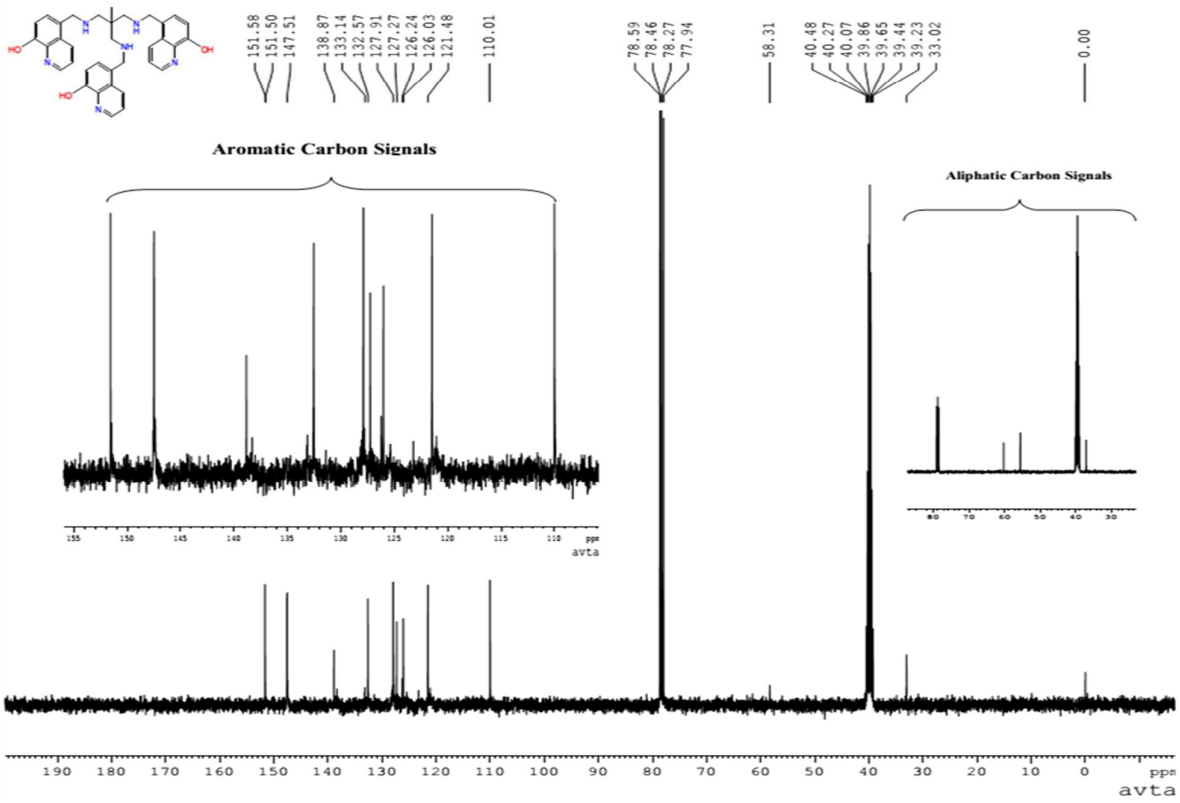

Figure 5: ^{13}C NMR spectrum of TAME5OX (DMSO, 300 MHz), insets showing chemical shifts due to aromatic carbons (left), and aliphatic carbons (right).

The theoretically calculated ^{1}H and ^{13}C NMR chemical shifts of TAME5OX obtained through DFT/B3LYP method have been compared with the experimental data in Figue 4, b and Table 1. The methyl protons showed singlet peak at 1.2 ppm. The methylene protons of spacer showed signals in the spectrum at 2.05 ppm due –CH_2 group attached to central unit carbon and at 2.47 ppm due –CH_2 group attached to 8–hydroxyquinoline unit. Five peaks at

6.8, 7.2, 7.6, 8.4 and 8.9 were calculated for the aromatic –CH protons of 8–hydroxyquinoline unit in contrast to experimental findings where only four signals were obtained for these protons. The double doublet appeared at 6.94 ppm in the experimental ^{1}HNMR spectrum of TAME5OX due to 2 –CH protons were calculated theoretically as two doublets separately at 6.8 and 7.2 ppm as shown in Figure 7b. In addition the experimentally observed peak for hydroxyl proton at 9.74 ppm, was calculated theoretically at 9.78 ppm which was found merged with aromatic protons of oxine group in both cases due to intramolecular hydrogen bonding. The calculated chemical shifts gave qualitative trends although the values are not in quantitative agreement with the experiment measurements, whereas the linearity in curves between the calculated ^{1}H and ^{13}C NMR values with their respective experimental values (Figure 6, a–b) gave a perfect correlation.

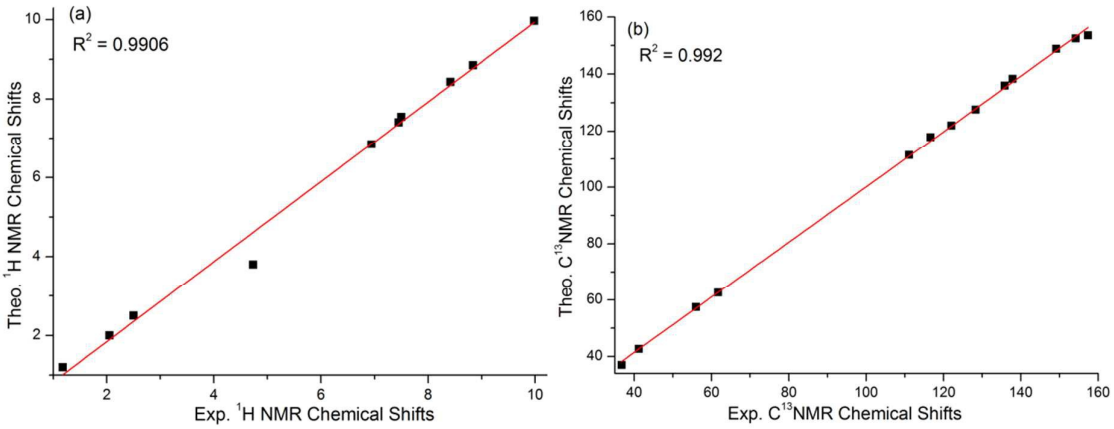

Figure 6: Correlation between the experimental and theoretical (a) ^{1}H NMR, and (b) ^{13}C NMR, data of TAME5OX.

3.1.3 Mass Spectra

High–resolution electrospray ionization time of flight mass spectrometry TOF MS(ES^{+}) was used to identify the product by evaluation of the molecular ion peak of TAME5OX (Figure

7). The spectrum of TAME5OX showed two peaks at m/Z 598.2(20%) and 599.3(10%) corresponding to the neutral $[M]^+$ and protonated $[M+H]^+$ form of ligand, respectively.

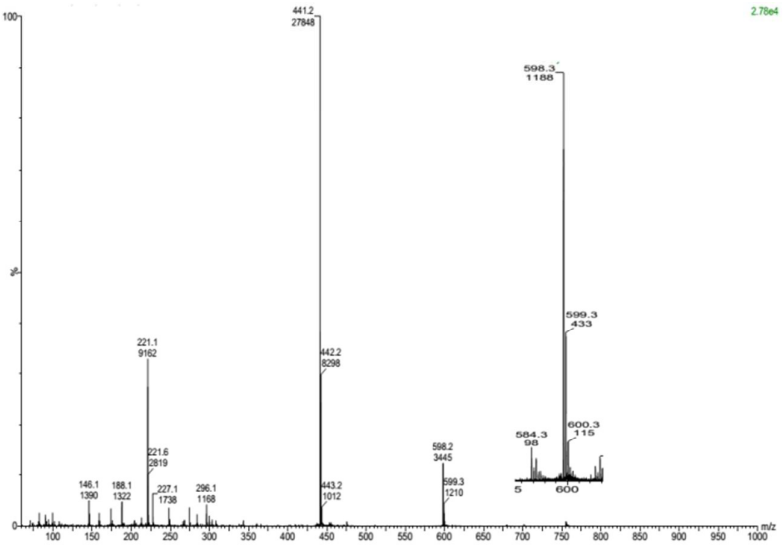

Figure 7: MS(ES+) mass spectrum of TAME5OX.

Table 1: Calculated (B3LYP/6–31G*) and Experimental (DMSO, 300 MHz) NMR (^{1}H and ^{13}C) Chemical Shifts (ppm), and IR Frequencies (KBr, cm^{-1}) for TAME5OX.

		NMR				IR	
Proton	B3LYP/631G*	Experimental	Carbon	B3LYP/631G*	Experimental	B3LYP/631G*	Experimental
H_1	1.18	1.2	C1	36.78	37.01	3619	3470
H_2	2.05	2.0	C2	41.23	42.65	2998	2932
H_3	2.5	2.4	C3	55.99	57.45	1649	1594
H_4	4.73	3.61	C4	61.72	62.66	1556	1454
H_5	7.45	7.41	C5	111.1	111.44	1383	1396
H_6	6.94	6.85	C6	116.65	117.88	1152	1239
H_7	7.5	7.55	C7	122.04	121.93	1087	1172
H_8	8.42	8.43	C8	128.31	127.57	1022	1080
H_9	8.84	8.85	C9	135.82	135.97		
H_9	9.98	9.74	C10	137.86	138.34		
			C11	149.14	148.87		
			C12	154.21	152.51		
			C13	157.39	153.58		

3.2 Ligand Properties: Thermodynamics and Spectrophotometry

3.2.1 Ligand Deprotonation Constants

In order to evaluate the competition between the protons and metal ions for the coordination sites, it was necessary to determine first the acid–base properties of the ligand. The deprotonation constants of TAME5OX were determined separately by potentiometry, UV–visible and luminescence spectrophotometry methods. Owing to insolubility of hexadentate ligand in water, it was dissolved in appropriate amount of standard 0.1M HCl to make it water soluble by converting into its hydrochloride salt. The neutral TAME5OX is addressed as LH_3, whereas the fully protonated form of TAME5OX is considered as a potentially nona–protic acid and is denoted as $(H_9L)^{6+}$. It possesses nine potential protonation sites: three phenolate oxygen atoms, three pyridine nitrogens and three secondary amine nitrogen atoms of pendant arms. The extracted pK_a values (protonation equilibria) obtained from titrations in the pH range 1.6–12.5, are defined by the following equations:

$$(H_{10-i}L)^{(7-i)+} \leftrightharpoons (H_{9-i}L)^{(6-i)+} + iH^+ \qquad (1)$$

$$K_{ai} = \left[(H_{9-i}L)^{(6-i)+}\right][\mathrm{H}^+]^{\mathrm{i}} \Big/ \left[(H_{10-i}L)^{(7-i)+}\right] \quad (i = 1-9) \qquad (2)$$

The potentiometric titration of the protonated form $(H_9L)^{6+}$ of the ligand was carried out in the p[H] range of 1.2–10.5 in 0.1 M KCl with NaOH at 25°C. Due to its poor solubility in water (as precipitation below pH 7.0 at concentration 1×10^{-3}M–1×10^{-4}M), the final concentration was maintained to 1×10^{-5}M and data were analyzed by the HYPERQUAD program.[28] Analysis of potentiometric curve (Figure 8) allowed the determination of nine deprotonation constants (the number in parentheses corresponds to the standard deviation in the last significant digit): log K_1 = 9.89(4), log K_2 = 8.92(5), log K_3= 8.42(4), log K_4 = 6.71(3), log K_5 = 6.38(2), log K_6 = 5.88(1), log K_7 = 4.60(2), log K_8 = 4.12(1) and log K_9 =

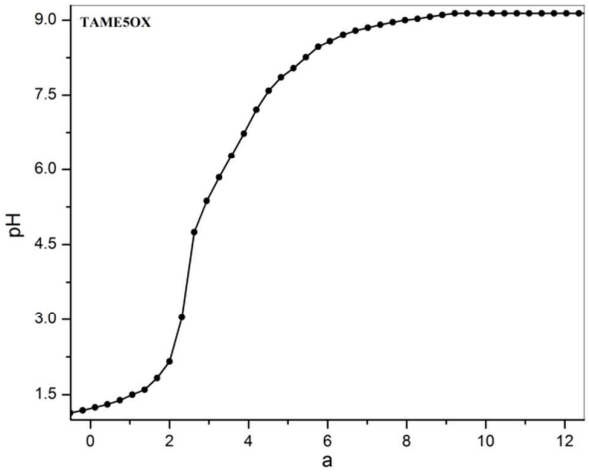

Figure 8: Potentiometric titration curve of TAME5OX (1×10^{-5}M). Solvent H_2O, I = 0.1M (KCl), T= 25(2)°C, and 'a' is the moles of base added per mole of TAME5OX present. Symbols and solid lines represent the experimental and calculated data, respectively.

3.64(6). UV–visible spectrophotometric titrations were also carried out showing three buffer regions in the pH range of 1.97–10.81: one, in the pH range of 1.97–6.69 ('a' of Figure 9; corresponding spectra exhibit three isosbestic points at 217, 250 and 272 nm), second region in the pH range 7.53–9.35 (Figure 11b, spectra exhibit three more isosbestic points at 277, 295 and 315 nm) and the third buffer region in the pH range 9.62–10.81 ('b' of Figure 9, spectra overlayed exhibit λ_{max} at 325nm). Analysis of spectrophotometric data performed by the program Hypspec[29] gave a model with same number of absorbing species (as observed by potentiometric titration) involving three proton exchange in each pH range and also nine deprotonation constants, which are in good agreement with that determined by potentiometric method.

In consideration to further support the number and nature of species obtained by both potentiometric and spectrophotometric methods and the corresponding deprotonation constants discussed above, luminescence titrations were also carried out for 1×10^{-5}M solution of TAME5OX from 1.97–10.81 pH range. The typical example of experimental data for the luminescence titration of the ligand is depicted in Figure 10. The best refinement of the

luminescence–pH data by the Hypspec program corresponds to the presence of nine species, in concurrence with the potentiometric and spectrophometric data; the values of Log Ks are returned in table 2 (the number in parentheses corresponds to the standard deviation in last significant digit).

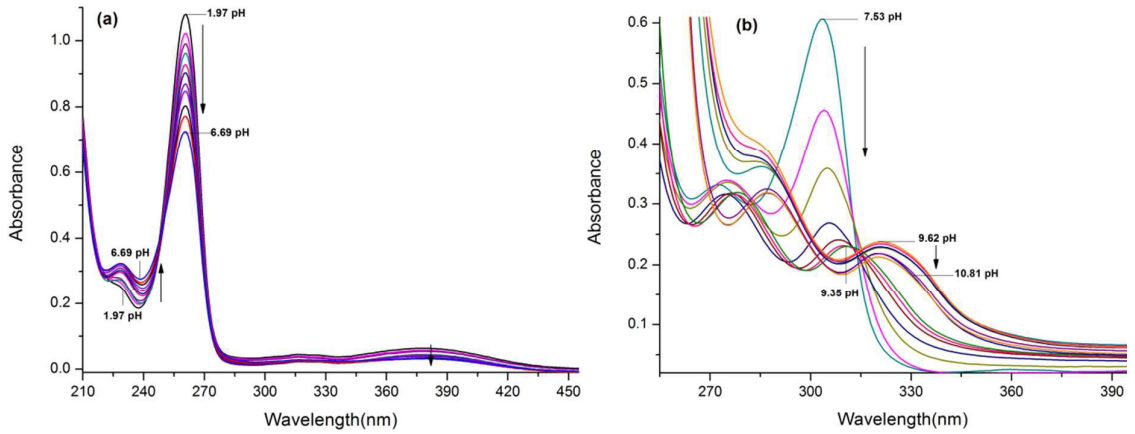

Figure 9: UV–vis absorption spectra of TAME5OX (1.0×10^{-5}M) as a function of pH: (a) pH = 1.97−6.69; (b) pH = 7.53−10.81. Solvent: H_2O, I = 0.1M (KCl), T = 25.0(2)°C.

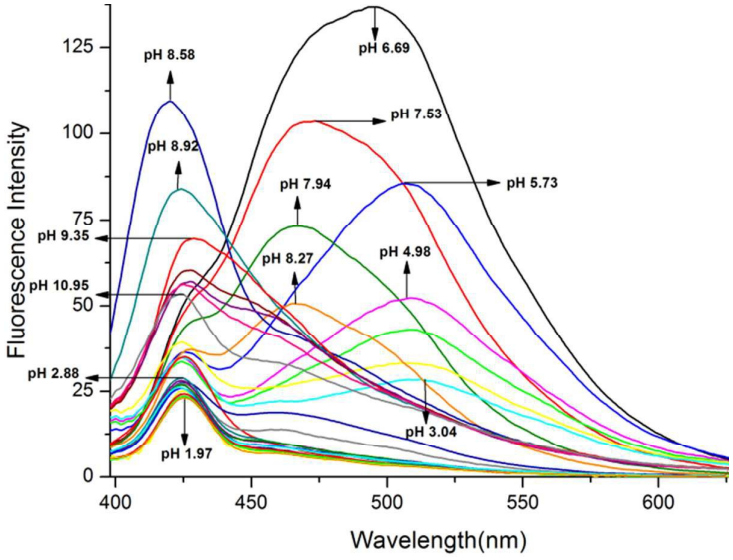

Figure 10: Dependence of the fluorescence emission spectra of aqueous solution of TAME5OX (1.0×10^{-5}M) on the change of the pH value from acidic to basic range (1.97–10.95 pH), T = 25.0(3)°C (excitation and emission slit widths of 5.0 nm) with an excitation wavelength of 385 nm.

Table 2. Protonation constants[a] (logK) of TAME5OX, (p = potentiometry, s = spectrophotometry and f = fluorometrically) and ligands containing 8–hydroxyquinoline subunits.

Ligand	log K_1	log K_2	log K_3	average log K_{1-3}	log K_4	log K_5	log K_6	average log K_{4-6}	log K_7	log K_8	log K_9	average log K_{7-9}
TAME5OX[b]	9.89(4)^p	8.92(5)^p	8.42(4)^p	9.07^p	6.71(8)^p	6.38(2)^p	5.88(4)^p	6.32	4.60(4)^p	4.12(2)^p	3.64(4)^p	4.12
	9.82(5)^s	8.97(4)^s	8.39(3)^s	9.06^s	6.79(7)^s	6.35(1)^s	5.82(3)^s	6.32	4.65(5)^s	4.08(1)^s	3.67(3)^s	4.13
	9.79(3)^f	8.87(6)^f	8.36(7)^f	9.00^f	6.63(3)^f	6.30(5)^f	5.80(1)^f	6.24	4.63(3)^f	4.16(1)^f	3.62(6)^f	4.13
Oxinobactin[c]	8.51(3)	7.78(2)	6.90(4)	7.73	4.07(7)	2.75(9)	2.28(2)	3.02	4.07(7)	2.75(9)	2.28(2)	3.02
Sulfoxinobactin[c]	7.84(1)	7.03(1)	6.18(2)	7.02	2.78	~2	1.42(3)	2.07	2.78	~2	1.42(3)	2.07
Tsox[b,d]	9.46(3)	8.44(4)	6.4(1)	8.1	4.4(1)	3.2(1)	1.8(1)	3.13	4.4(1)	3.2(1)	1.8(1)	3.13
TsoxMe[b,d]	9.19(7)	8.20(9)	6.65(11)	8.01	3.94(14)	-	-	-	3.94(14)	-	-	-
O–TRENSOX[b,e]	8.62	8.18	7.44	8.08	3.01	2.55	1.83	2.46	3.01	2.55	1.83	2.46

a Numbers in parentheses represent the standard deviation in the last significant digit. b In water (I = 0.1M KCl). c In methanol/water (80/20 w/w, I = 0.1M NaClO4). c Reference [30]. d Reference [32]. e Reference [31].

All constants are reported in Table 2 together with some similar ligands containing 8–hydroxyquinoline or its sulphonate derivative (oxinobactin, sulfoxinobactin),[30] (TMOM5OX)[19] and (O–TRENSOX)[31] based on the backbone of tris(2–aminoethyl)amine); the structures of these ligands are also given in Figure 2 for comparison. The three highest log K values found between 8.42 and 9.89 and three lowest values between 3.64 and 4.60 are assigned to the deprotonation of the hydroxyl and pyridinium nitrogen moieties of the three quinolinate groups, respectively, whereas the log K between 5.88 and 6.71 were attributed to the secondary amines for these ligands. Inspite of the differences in solvents or other experimental conditions, the log K values of TAME5OX and these reported ligands can be compared: the average value for the log K of the oxygen sites, 9.07 for TAME5OX, is much higher than the corresponding value (7.73 for oxinobactin, 7.02 for sulfoxinobactin, 8.08 for O–TRENSOX and 8.65 for Tsox). The same trend was observed for protonation of the nitrogen sites: the average value is 4.45 for TAME5OX and (3.02 for oxinobactin, 2.07 for sulfoxinobactin, 2.46 for O–TRENSOX and 3.01 for Tsox). This differences seems to be due to the absence of an electron withdrawing effects of sulphonate group in case of oxinobactin and sulfoxinobactin[30] and carbonyl group of amide linkage at ortho position to hydroxyl moieties.[31,32] The higher values of TAME5OX could be due to electron donating

effect of CH_2–NH–CH_2 linkage attached at 5–position (para to hydroxyl group) of 8–hydroxyquinoline. Moreover, the deprotonation constant (log K) ranges for the nitrogen and oxygen atoms differ from the statistical factor of (log 4 = 0.6), which points to cooperativity taking place between the three arms of the tripodal ligand, probably via intra– or intermolecular hydrogen bonds, similar to the situation for oxinobactin and Tsox, but in contrast to O–Trensox.

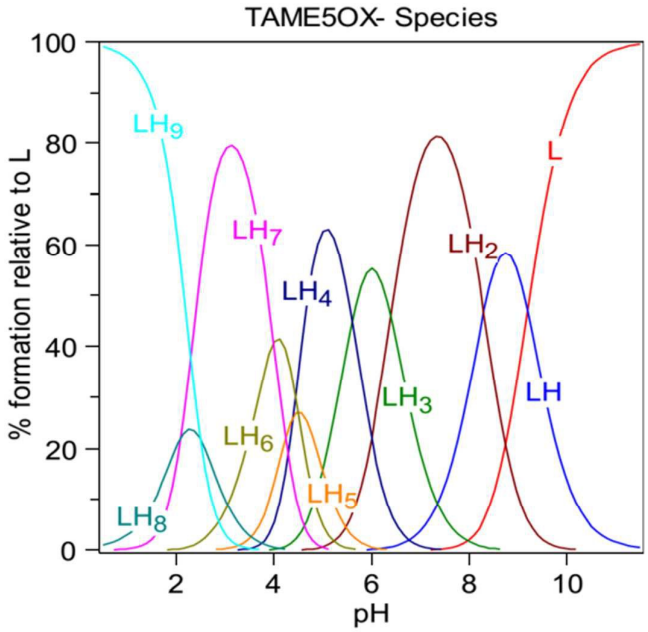

Figure 11: Species distribution curves of TAME5OX containing species, computed from the protonation constants given in Table 2. Calculated for $[TAME5OX]_{tot} = 1\times10^{-5}$ M, Solvent : H_2O, I = 0.1M (KCl), T = 25.0(2)°C.

The corresponding distribution curves of TAME5OX obtained from the log K values are presented in Figure 11 which indicate that in acidic solution TAME5OX initially exists 100% in the fully protonated form as LH_9 below pH 2.9. As the pH is increased, deprotonation starts, the ligand loses two protons subsequently from the N–pyridyl of oxine unit with formation of LH_8 and LH_7 which exist between pH 0.8–4.0 and 1.2–4.8 with maximum concentration of 28% and 81% at pH 2.8 and ~3.4 respectively. Further release of protons lead formation of LH_6, LH_5 and LH_4 successively in the pH range of 2.9–6.5 with maximum

concentration 42%, 49% and 63% at pH 4.1, 4.8 and 5.2, respectively. Further deprotonation leads to the formation of LH_3, the neutral form of TAME5OX, in pH range of 4.9–7.4 with maximum concentration 57% at pH 6.3. Other species LH_2 and LH were formed after pH 5.2 and 7.5, with maximum concentration of 82% and 61%, respectively. No isosbestic points in the electronic spectra ('b' Figure 10) were observed above the pH 9.62 and the spectra overlapped with each other.The fully deprotonated ligand (L) was predominant above pH 9.0 with 100% concentration.

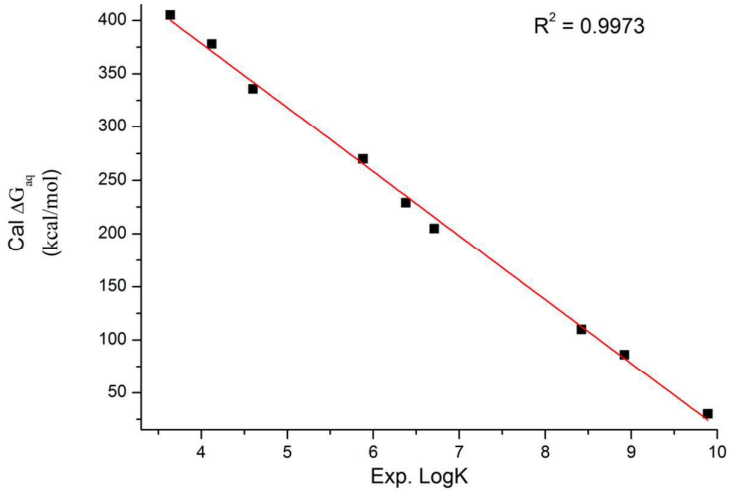

Figure 12: Correlation between the experimental log K and calculated ΔGº of TAME5OX.

In order to validate the assignment of experimental protonation constants, aqueous–phase free energy for the entire representative species of TAME5OX were calculated by density functional theory by B3LYP/6-31G* quantum mechanical approach. For an acid species AH, the pK_a defined as the negative logarithm of the dissociation constant of the reaction $AH = A^- + H^+$, is given by the thermodynamics relation $pK_a = \Delta G_{aq,AH}/2.303\ RT$. The change in free energy in aqueous–phase is obtained according to the following equation:

$$\Delta G_{aq,AH} = \left(G_{aq,A^-} + G_{aq,H^+}\right) - G_{aq,AH} \qquad (3)$$

For which the proton free energy at 298 K and 1 atm is:

G_{aq,H^+} = 2.5RT−TΔS° =1.48−7.76

= – 6.28 kcal=mol

The greater acidity belongs to the group in which its hydrogen release is easier and there must be a decrease in ΔG values in the deprotonation process. A clear decrease in ΔG was observed in case of TAME5OX (Figure 12) as the deprotonation take place from protonated N– of 8–hydroxyquinoline from fully protonated free ligand, LH_9^{6+}, followed by protonated amines of pendant arms and hydroxyl groups of binding units. The validity of this theoretically calculated ΔG_{aq} for the different species of TAME5OX was compared with the calculated experimental pK_a, which resulted an acceptable correlation with R^2 = 0.98956.

3.2.2 Absorption spectra of ligand (TAME5OX) and its protonated species

The ligand TAME5OX shows two peaks 255 and 310 nm (ε = 110, 000 $M^{-1}cm^{-1}$ and 60, 100 $M^{-1}cm^{-1}$, respectively) in the UV-visible region assigned to π→π* and n→π* transitions. Since, a variety of species are formed with change on pH, the large spectral changes (Figure 9, a–b) observed in the spectrophotometric titration of the TAME5OX as a function of pH is indicative of a change in the protonation and deprotonation behaviour of the ligand. At pH ≤ 2.9, the electronic spectrum of the TAME5OX in its protonated form is symbolized by a strong absorption band at higher energies 263 nm, (ε = 110, 000 $M^{-1}cm^{-1}$) assigned for π→π* transitions and a broad band at 380 nm, (ε = 5, 000 $M^{-1}cm^{-1}$) assigned for n→π* transition, respectively. Upon rising pH above 2.9, the deprotonation of the pyridinium nitrogen results in hypochromic shifts (263 nm, ε = 72,000 $M^{-1}cm^{-1}$ and 380 nm, ε = 2, 300 $M^{-1}cm^{-1}$) with the simultaneous ascent in absorbance towards lower wavelength, 230 nm (ε =32, 000 $M^{-1}cm^{-1}$) which results in the formation of three isosbestic points at 217, 250 and

272 nm as shown in Figure 9 . The isosbestic points assert the formation of three protonated species of the ligand in the pH range of 1.97–6.69, consequently which can be well comprehended from species distribution curves (Figure 11).

Above pH 6.7, the deprotonation of protonated secondary amines of TAME5OX, is characterized by a main absorption band centered at 308 nm, (ε = 60, 100 $M^{-1}cm^{-1}$) with a shoulder at about 279 nm, (ε =38, 000 $M^{-1}cm^{-1}$) attributed to n→π* and π→π* transitions, respectively, and the broad band around 380 nm get diminished in this pH range ('b' of Figure 9). The deprotonation results in the bathochromic and hypochromic shifts with the rise of pH from acidic to neutral medium. The formation of three more isosbestic points at 276 nm, 295 nm and 315 nm, confirms the formation of LH_6, LH_5 and LH_4 species, respectively. Similarly, under basic conditions the electronic spectra of ligand exhibits two bands, one at higher energies was red shifted (about 17 nm) to 325 nm, (ε = 28, 000 $M^{-1}cm^{-1}$) and low energy band was also hyperchromically red shifted (about 14 nm) to 290 nm, (ε = 40, 000 $M^{-1}cm^{-1}$) (Figure 9), and evidenced the deprotonation of hydroxyl function from neutral form (LH_3) of TAME5OX to form LH_2, LH and L upon variation of pH upto 10.81. Bands at λ > 300 nm have attributed to n→π* state with charge–transfer character while the band around 285 nm concerns the quinoline ring.[31] It should be noticed that the band due to protonation of N_{py} disappears in this pH range. No spectral change was observed on further pH variation upto 11.5.

To corroborate the above argument for the deprotonation behavior of ligand, the electronic spectra of different species of TAME5OX obtained were calculated by time–dependent density functional theory (TD–DFT) at the B3LYP/6–31G* level. The calculated spectra for the neutral (LH_3), protonated and deprotonated species (LH_9, LH_8, LH_7, LH_6, LH_5, LH_4 and LH_2, LH) were obtained by stepwise protonation and deprotonation of N–, NH– and OH– groups, respectively (Figure 13). The experimental spectra of TAME5OX

gave major variations for the π–π* transition; the peak of protonated (LH_9, LH_8 and LH_7) at 262 nm ('a' of Figure 13) shifted bathochromically with formation of LH_6, LH_5 and LH_4, show transitions at 274, 276 and 278 nm, respectively. Similar variations were also observed in the calculated electronic spectra ('b' of Figure 13) and the corresponding calculated values

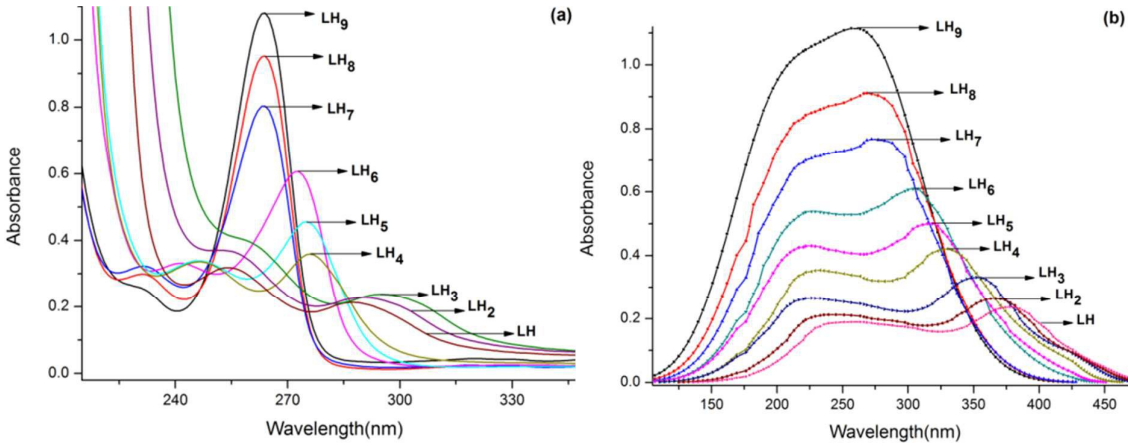

Figure 13: pH–dependent electronic spectra (absorption) of the nine species as a function of molar absorptivity and wavelength (a) predicted from Hypspec using experimental data and (b) calculated through TD–DFT/B3LYP method by employing 6–31G* basis set, for the protonation and deprotonation of ground state geometrical optimized neutral species (LH_3) of TAME5OX.

are reported in table 3. The calculated π–π* and n–π* transitions for the LH_6, LH_5 and LH_4 obtained at 245 nm and 280 nm, shifted to 260 nm and 300 nm for the species LH_3, LH_2 and LH respectively. The simulated electronic absorption spectra for corresponding predicted species are in good concurrence in the contour, number of absorption bands and relative intensities with the species except small red–shifts in LH_3, LH_2 and LH forms, which are due to the impossibility of considering all the symmetrical orbitals in TD–DFT calculation. Also, strong absorption peaks were obtained from theoritical calculations at 264 nm for LH_9 and at the same position with comparatively lower intensities for LH_8 and LH_7 species, which corroborates well with the experimental results.

Table 3: Computed Optical Properties: Absorption–S0 and emission–S1; wavelengths, oscillator strengths (f_{calc}), electronic transitions and energies calculated at the TD–DFT/6–31G* level of theory, using DFT/B3LYP and DFT/cam–B3LYP for ground state and excited state geometry, respectively, for different species of the TAME5OX.

	S0				S1			
Species	**λ_{nm} (abs)**	**f_{calc}**	**Nature**	**Transition (Excitation energy)**	**λ_{nm}(em)**	**f_{calc}**	**Nature**	**Transition (Emission energy)**
$(H_9L)^{6+}$	270.54	0.3281	HOMO-2→LUMO+1	110→114 (1.186 eV)	425.64	0.1091	HOMO-1→LUMO+1	111→114 (0.162 eV)
$(H_8L)^{5+}$	272.34	0.1794	HOMO-1→LUMO	111→113 (0.883 eV)	425.89	0.1581	HOMO→LUMO+1	112→114 (0.293 eV)
$(H_7L)^{4+}$	274.89	0.1563	HOMO-2→LUMO	110→113 (0.726 eV)	519.95	0.1674	HOMO-2→LUMO	110→112 (0.385 eV)
$(H_6L)^{3+}$	220.84 310.23	0.1068 0.0921	HOMO-1→LUMO HOMO→LUMO	111→113 (0.590eV) 112→113 (0.513 eV)	522.83	0.1748	HOMO-1→LUMO	111→112 (0.571eV)
$(H_5L)^{2+}$	223.60 319.37	0.0821 0.0731	HOMO→LUMO+1 HOMO-1→LUMO	112→ 114 (0494 eV) 111→113 (0.489 eV)	526.64	0.1921	HOMO-1→LUMO	111→ 112 (0.836 eV)
$(H_4L)^{+}$	225.30 337.42	0.0675 0.0598	HOMO-1→LUMO+2 HOMO-1→LUMO	111→115 (0.314 eV) 111→113 (0.379 eV)	528.93	0.2107	HOMO→LUMO+1	112→114 (1.243 eV)
(H_3L)	229.91 350.42	0.0401 0.0463	HOMO-2→LUMO+1 HOMO→LUMO	110→114 (0.253 eV) 112→113 (0.288 eV)	530.37	0.2193	HOMO-1→LUMO+1	111→114 (1.391 eV)
$(H_2L)^{-}$	234.98 372.87	0.0374 0.0412	HOMO-1→LUMO+1 HOMO→LUMO	111→114 (0.192 eV) 112→113 (0.219 eV)	474.67	0.2116	HOMO→LUMO	112→113 (1.287 eV)
$(HL)^{2-}$	244.26 376.05	0.0283 0.0403	HOMO-1→LUMO HOMO→LUMO	111→113 (0.175 eV) 112→113 (0.209 eV)	470.23	0.1875	HOMO-1→LUMO	111→113 (0.723eV)
$(L)^{3-}$	245.16 379.08	0.0138 0.0294	HOMO→LUMO+1 HOMO→LUMO	112→114 (0.159 eV) 112→113 (0.184 eV)	429.34	0.1845	HOMO-2→LUMO	110→113 (0.596 eV)

3.2.3 Fluorescence Spectra of ligand (TAME5OX)

In general, the binding moiety of 8–hydroxyquinoline serves as a fluorophore because of the significant enhancement of fluorescence that is known to occur when the excited state intramolecular proton transfer (ESIPT) between the hydroxyl group and quinoline nitrogen is suppressed upon binding of a metal cation.[33] However, some HQ derivatives are poorly luminescent[34] due to an intramolecular photoinduced proton transfer (PPT) process between the hydroxyl group (which is relatively strong photoacid) and the nearby quinoline nitrogen (which is, in turn, a strong photo base). In addition, in protic media, intermolecular PPT process involving solvent molecules can also occur, further decreasing the fluorescence quantum yield of this kind of fluorophore. The 8–hydroxyquinoline ligands are indeed

characterized by strong intramolecular hydrogen bonding that may be photoinduced to undergo proton transfer in the excited state.[35,36]

In the present tripodal ligand containing three units of 8–hydroxyquinoline, upon excitation into the ligand transitions, a maximum of emission at about 425 nm was observed (Figure 10). This fluorescence emission originates from an excited–state intramolecular proton transfer (ESIPT), and enhanced fluorescence with absolute quantum yield ≈0.091) may be attributed to presence of three units of 8–hydroxyquinoline in TAME5OX.

3.2.3.1 pH–Dependent Fluorescence Spectra

From survey of pH-dependent photophysical properties of 8-hydroxyquinoline compounds, it is seen that, the fluorescence intensity of these compounds changes in a monotonous way, depending only on the change of pH, which gets increased or decreased along with the change in the pH value in a consistent way due to the only one photoinduced electron transfer mechanism between pyridyl –N and –OH group of quinoline unit, resulting in the OFF–ON or ON–OFF type of fluorescent pH sensors.[37] Moreover, there are reports on the pH sensors based on the opposite photoinduced electron transfer processes between a receptor and signaling unit.[38] To explore the pH–dependent optical properties of TAME5OX with unique pyridyl–N and –OH structural characteristics, the pH vs fluorescence titration experiment was carried out in aqueous medium. An appropriate volume of 0.1M HCl and 0.1M NaOH were used for protonation of pyridyl –N group and deprotonation of the –OH group, respectively. As shown in Figure 9, the π–π* and n–π* transitions in the electronic absorption spectrum of TAME5OX exhibit the exemplary behaviour (red and hypochromic shifts) along with changing the pH of the system from acidic to basic (as discussed in protonation of TAME5OX). In good comparison, the changes in the blue–green emission of the ligand maxima located at 425 nm which was excited at 385 nm, were monitored as a function of pH ranging from 1.97–10.81 (Figure 10) at room temperature. The emission

intensity at 425 nm (with meagre quantum yield) as well as maximum wavelength remains almost unchanged, no substantial change in behaviour of the fluorophore was observed upon measuring emission under acidic conditions within the pH range of 1.97–2.88. Most interestingly, with an increase in the pH from 3.04 to 6.69, resulted the evolution of emission peak at 520 nm upto ~5 fold (could be attributed to the competition between the intramolecular photon induced proton transfer), while no change in blue–green emission at 425 nm. Further rise of pH resulted the intense fluorescence of TAME5OX gradually get blue shifted (about 50 nm) towards 470nm, along with quenching of fluorescence signal about 1, 2 and 3–fold at 7.53, 7.94 and 8.27 pH, respectively. After addition of more base (0.1M NaOH) (pH > 8.5), the deprotonation effect again evidenced in growth of fluorescence signal upto 3–fold which promptly got blue shifted to original blue–green emission wavelength (420 nm). Surprisingly, with an increase in the pH from 8.9 to 10.9, the intense fluorescence of the same compound under basic conditions also gets gradually quenched in a similar manner as observed under acidic conditions, (cf. Figure 10). It is worthnoting that more significant changes under physiological pH and less significant changes under acidic and basic medium confirm that protonation of N atom lowers the LUMO energy and decreases the vertical S1→S0 transition energy, and the deprotonation of the hydroxyl function also destabilize the HOMO, thus closing the gap giving rise to smaller transition, while in neutral form the HOMO–LUMO gap increases which corresponds significant red shifts along with intense fluorescence. Thus, among all the species formed during the pH range of 1.8–10.9, the neutral species, LH_3, was found to be more fluorescent that predominates under physiological pH, while the more protonated and deprotonated species were found to be less fluorescent.

These results divulge the typical characteristics of a pH–fluorescent probe through the photoinduced proton transfer (PPT) enhancement process and photoinduced electron transfer (PET) quenching processes between pyridyl–N and –OH group for this tripodal chelator.[34,38]

In other words, these two processes between the 8–HQ receptor units are accountable for the particular fluorescent properties in TAME5OX ligand along with either decreasing the pH from 6.7 to 1.97 or increasing the pH from 6.9 to 10.88. The unique pH–dependent fluorescent property of this ligand indicates the potential application, as pH indicator under both acidic as well as basic conditions, and, will act as novel OFF–ON–OFF type of fluorescent pH sensor.

3.2.3.2 pH–Dependent PET and PPT Mechanisms

For the intention of cognizance the remarkable pH–dependent fluorescence characteristics of TAME5OX, the following PET quenching and PPT enhancement mechanisms determined by the orbital energy levels of the excited states of 8–HQ unit of the ligand is presented at Figure 14. In principle, 8–HQ unit can serve as both electron donor and acceptor upon photoexcitation, i.e., the photoinduced electron can transfer from the excited pyridyl–N moiety to the lowest unoccupied molecular orbital (LUMO) of the –OH group (donor–excited PET; d–PET) or just reversely from the highest occupied molecular orbital (HOMO) of –OH to the excited pyridyl–N moiety (acceptor excited PET; a–PET).[39] When the N atom is protonated in the form of NH^+, the LUMO energy of electron deficient 8–HQ unit becomes lower than that of the excited aromatic ring, (see left part of. Figure 14), leading to a d–PET quenching process. In contrast, when the OH group of 8–HQ is deprotonated into O^-, the HOMO energy of aromatic ring gets increased and becomes higher than that of excited N atom, (right part of Figure 14) which induces the electron transfer from –OH moiety to pyridyl–N unit, giving rise to a reductive a–PET. These two opposite photoinduced electron transfer processes are in turn responsible for the special fluorescence characteristics of TAME5OX along with the change in the pH value under acidic and basic conditions,

resulting in a novel OFF–ON–OFF type of pH fluorescent switch to acidic and basic conditions, respectively.

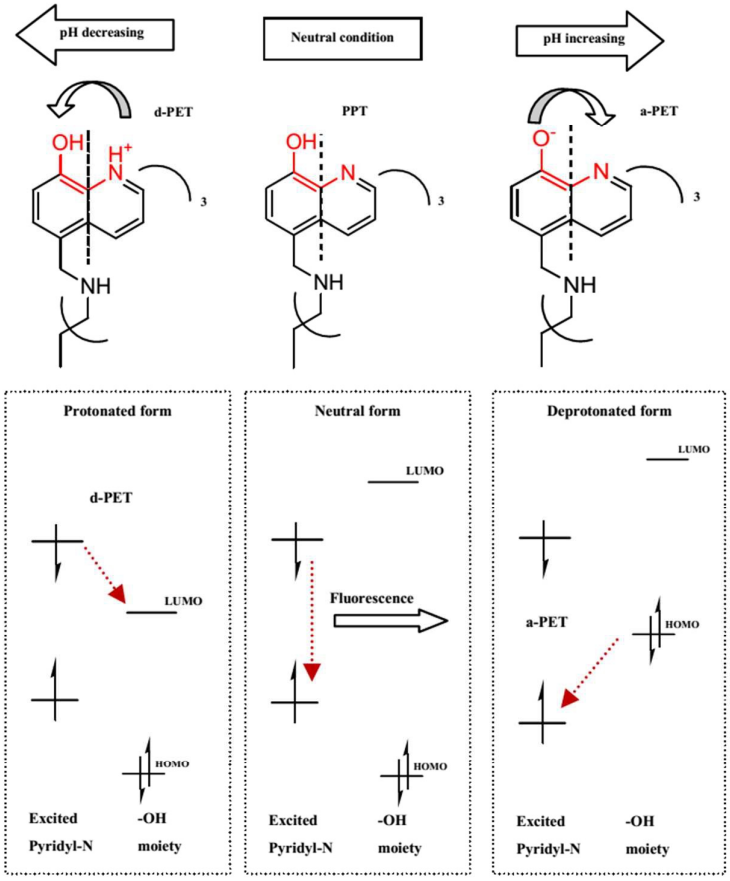

Figure 14: Proposed photoinduced electron transfer (PET) and photoinduced proton transfer (PPT) mechanisms between N–pyridyl and –OH groups of 8–HQ moieties of TAME5OX in protonated quinolinium, neutral, and deprotonated quinolinate states, respectively.

The above–mentioned two processes (PPT and PET) observed during pH dependent fluorescence of TAME5OX are clearly validated by density functional (DFT) calculation with the camB3LYP/6–31G* method based on the excited state optimized molecular structure of the ligand. The calculated frontier molecular orbital (MO) energies and surfaces of protonated, neutral and deprotonated species of TAME5OX are shown in Figure 15. The highest occupied π orbital (HOMO) is mainly located on phenolate side and the lowest unoccupied π* orbital (LUMO) is mainly located on the pyridyl moiety. As can be found,

both the HOMO and LUMO of TAME5OX in the neutral state are located almost completely on the aromatic side of 8–HQ moiety, while the HOMO-1 and LUMO+1 are located mainly on the –N pyridyl and hydroxyl group of 8–HQ unit, respectively. As a result, the electronic transition between HOMO and LUMO, leading to fluorescence from the π system of this compound.

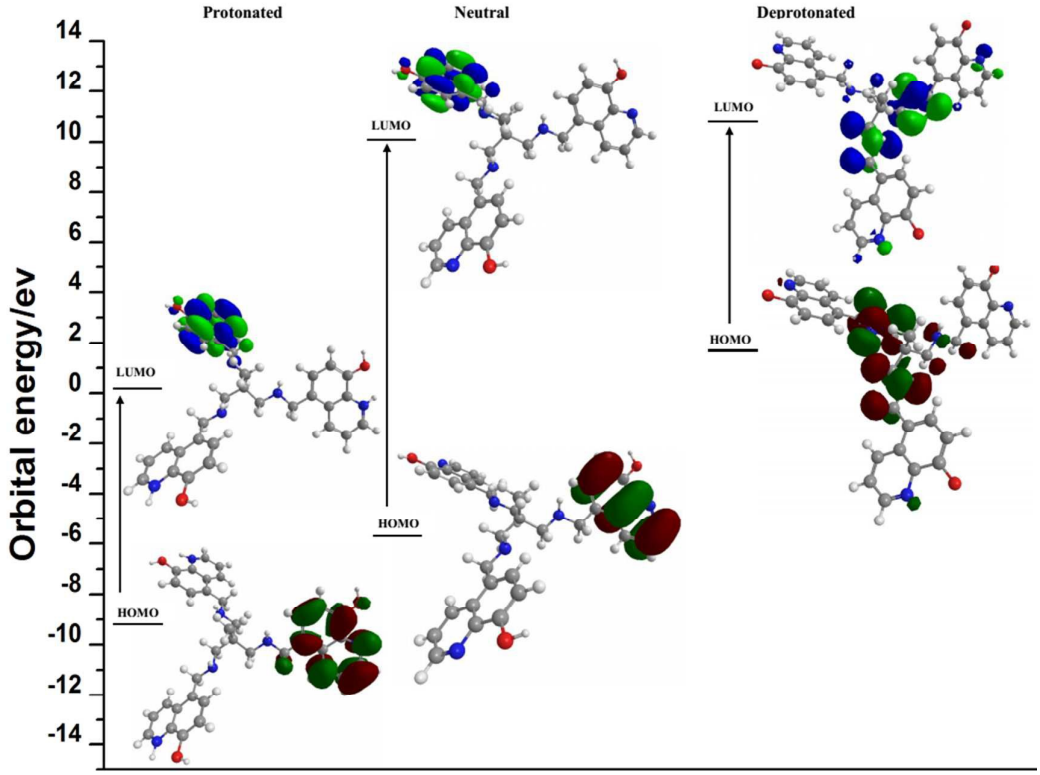

Figure 15: Calculated CAM–B3LYP/6−31G* energy levels and surfaces of frontier molecular orbitals (MOs) of TAME5OX in protonated, neutral, and deprotonated states, respectively.

When the N atom of 8–HQ in TAME5OX is protonated in the form of NH^+, the LUMO energy of pyridyl moiety, 1.168eV, becomes higher than that for the aromatic part in the molecule, 0.385eV, which in turn results in the electron transfer towards π system in moiety under neutral conditions as shown in Figure 15. When the OH group of the 8–HQ moiety of TAME5OX is deprotonated into O^- in the basic system, change occurs in the molecular structure of this compound. Along with structural change, the HOMO energy of the 8–HQ

moiety in the molecule gets increased to be close to those of the LUMO, which in turn decreases largely from that of π system of moiety, which decreases the energy gap and quenches the fluorescence intensity. For a better interpretation, the trends of the results are plotted in Figure 16, i,e; computed vertical S1→S0 emission energies (that is, fluorescence) are, as , maxima emission wavelength at 425 nm of highly acidic and basic species remains unchanged and the calculated emission data is reported in table 3. Other protonated and neutral (LH_3) forms are red−shifted by ca. 95 nm with significant enhancement of fluorescence intensity along stepwise deprotonation from LH_7 to LH_3, while deprotonated species LH_2 and LH show blue shifts with respect to the corresponding neutral emission value with decreasing intensity from LH_2→L, in good agreement with experimental results.

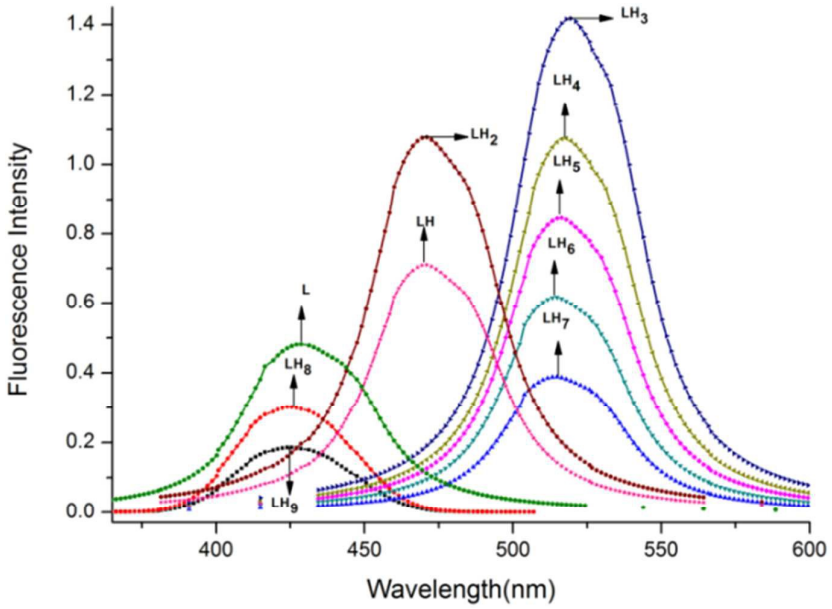

Figure 16: TD−camB3LYP simulated emission spectra of TAME5OX as a function of protonation and deprotonation of excited state geometrical optimized neutral species (LH_3) of by employing 6−31G* basis set.

3 Conclusion

The new and novel C_3 symmetric tripod, TAME5OX, derived from three bidentate 8−hydroxyquinoline subunits with nine donor atoms (three O and six N) has been

successively developed. The TAME5OX have been designed with the $-CH_2-NH-CH_2-$ connection in the para position with respect to the hydroxyl group of oxine sub-units. The results of UV–visible and luminescence studies reveal the special pH dependent behaviour of TAME5OX. The intense intrinsic fluorescence of TAME5OX gets diminished under acidic and basic conditions, due to the formation of protonated quinolinium $NH^+\sim-OH$ and deprotonated quinolinate $N\sim-O^-$ forms of the 8-HQ moiety, respectively, which leads to a photoinduced electron transfer from the excited N-pyridyl to 8-OH group and the just opposite process. This renders this compound the special OFF–ON–OFF type of pH-dependent fluorescent sensor. The time dependent density functional theory (TD–DFT), reveals the good agreement with the available experimental data. From a mechanistic point of view, the absence of fluorescence of TAME5OX in acidic as well as basic pH experimentally observed and claimed to be related to the the excited-state intramolecular proton transfer (ESIPT), from 8-OH to the quinolino-N atom was here proven and validated. Nevertheless, we have demonstrated, that the DFT calculations reveals the effect of molecular structure (actualy the 8HQ receptor unit edifice in tripodal architect) on the intrinsic fluorescent property and in turn the pH–sensing properties of this compound. The excellent photophysical properties of analouge make it a very good candidate with potential applications in chemical and biological fields and procedure followed in this investigation could provide valuable help in finding the most favourable channel and give suggestions in designing optical pH based sensors to detect trivalent metal ions in biological systems.

Supplementary Information

Detailed synthesis preocedure of tame, Cartesian coordinates of different species of TAME5OX and their dispersion corrected energied are provided.

Acknowledgements

One of the authors (B. K. Kanungo) acknowledges financial support from the department of science and technology (DST), New Delhi with grant No. $SR/S_1/IC\text{-}17/2011$ dated 30/04/2012; Rifat Akbar is thankful to the authorities of Sant Longowal Institute of Engineering and Technology, Longowal for providing financial assistance.

References:

[1] J. P. Phillips, *Chem. Rev.*1956, **56**, 271–297.

[2] (a) E. Bardez, I. Devol, B. Larrey, B. Valeur, *J. Phys. Chem. B,* 1997, **101**, 7786-7793;

(b) C. Lee, W. Yang, R. G. Parr, *Phys. Rev. B*, 1988, **37**, 785-789.

[3] M. D. Shults, B. Imperiali, *J. Am. Chem. Soc.*, 2003, **125**, 14248-14249.

[4] R. T. Bronson, D. J. Michaelis, R. D. Lamb, G. A. Husseini, P. B. Fransworth, M. R. Linford, R. M. Izatt, J. S. Bradshaw, P. B. Savage, *Org. Lett.*, 2005, **7,** 1105-1108.

[5] F. Launay, V. Alain, E. A. Destandau, N. Ramos, E. A. Bardez, P. Baret, J. L. Pierre, *New J. Chem.*, 2001, **25**, 1269-1280.

[6] S. Y. Moon, N. R. Cha, Y. H. Kim, S. K. Chang, *J. Org. Chem., 2004,* **69**, 181–183

[7] V. A. Montes, G. Li, R. Pohl, J. Shinar, P. Anzenbacher, *Adv. Mater.*, 2004, **16**, 2001-2003.

[8] G. Farruggia, S. Iotti, L. Prodi, M. Montalti, N. Zaccheroni, P. B. Savage, V. Trapani, P. Sale, F.I. Wolf, *J. Am. Chem. Soc.,* 2006, **128**, 344–350.

[9] M. Shirakawa, N. Fujita, T. Tani, K. Kaneko, S. Shinkai, Chem. Commun., 2005, **33**, 4149–4151.

[10] I. M. Kolthoff, E. B. Sandell, Textbook of quantitative inorganic analysis, Macmillan, New York, NY, 1952.

[11] H. L. Zheng, L. M. Weiner, O. Bar-Am, S. Epsztejn, Z. I. Cabantchik, A. Warshawsky, N. B. H. Youdim, M. Fridkin, *Bioorg. Med. Chem.*, 2005, **13,** 773–783.

[12] X. Guo, X. Qian, L. Jia, *J. Am. Chem. Soc.,2004,* **126**, 2272-2273.

[13] Y. Mei, P. A. Bentley, W. Wang, *Tetrahedron Lett.,* 2006, **47**, 2447–2449.

[14] C. H. Chen, J. Shi, Coord. Chem. Rev., 1998, **171**, 161–174.

[15] L. D. Loomis, K. N. Raymond, *Inorg. Chem.,* 1991, **30**, 906–911.

[16] F. L. Javier, N. Cristina, N. F. Olalla, L. C. Jose, L. Carlos, J. S. Seixas de Melo, S. L. Carlos, *Inorg. Chim. Acta.*, 2012, **381**, 218–228.

[17] R. D. Hancock, *J. Chem. Educ.*, 1992, **69**, 615–621.

[18] C. Perez–Bolivar, V. A. Monstes, P. Anzenbacher, *J. Inorg. Chem.*, 2006, **45**, 9610–9612.

[19] A. Rifat, B. Minati, B. K. Kanungo, *Spec. chim. Acta Part A,* 2014, **129**, 365–376.

[20] A. Rifat, B. Minati, B. K. Kanungo, *J. Photochem. Photobi. A*, 2014, **287**, 49–64.

[21] L. Lihua, X. Bing, *Tetrahedron*, 2008, **64**, 10986–10995.

[22] B. Laurence, D. Lionel, A. F. Noels, *Tetrahedron,* 2007, **63** (2007) 7003–7008.

[23] (a) S. Grimme, J. Antony, S. Ehrlich, H. Krieg, J. Chem. Phys., 2010, **132**, 154104–154122; (b) Gaussian 09, Revision A.01, M. J. Frisch, G.W. Trucks, H. B. Schlegel, G. E. Scuseria, M. A. Robb, J. R. Cheeseman, G. Scalmani, V. Barone, B. Mennucci, G. A. Petersson, H. Nakatsuji, M. Caricato, X. Li, H. P. Hratchian, A. F. Izmaylov, J. Bloino, G. Zheng, J. L. Sonnenberg, M. Hada, M. Ehara, K. Toyota, R. Fukuda, J. Hasegawa, M. Ishida, T. Nakajima, Y. Honda, O. Kitao, H. Nakai, T. Vreven, J. A. Montgomery, Jr., J. E. Peralta, F. Ogliaro, M. Bearpark, J. J. Heyd, E. Brothers, K. N. Kudin, V. N. Staroverov, R. Kobayashi, J. Normand, K. Raghavachari, A. Rendell, J. C. Burant, S. S. Iyengar, J. Tomasi, M. Cossi, N. Rega, J. M. Millam, M. Klene, J. E. Knox, J. B. Cross, V. Bakken, C. Adamo, J. Jaramillo, R. Gomperts, R. E. Stratmann, O. Yazyev, A. J. Austin, R. Cammi, C. Pomelli, J. W. Ochterski, R. L. Martin, K. Morokuma, V. G. Zakrzewski, G. A. Voth, P. Salvador, J. J. Dannenberg, S. Dapprich, A. D. Daniels, O. Farkas, J. B. Foresman, J. V. Ortiz, J. Cioslowski, and D. J. Fox, Gaussian, Inc., Wallingford CT, 2009.

[24] E. B. Fleischer, A. E. Gebala, A. Levery, P. A. Tasker, *J. Org. Chem.,* 1971, **36**, 3042–3044.

[25] J. Burckhalter, R. I. Leib, *J. Org. Chem.,* 1961, **26**, 4078–4083.

[26] S. K. Chatterjee, N. D. Gupta, *J Poly Sci. Part A-I.* 1973, **11**, 1261−1270.

[27] M. Albrechet, K. Witt, R. Frohlich, O. Kataeva, *Tetrahedron,* 2002, **58**, 561−567.

[28] L. Al derighi, P. Gans, A. Ienco, D. C. Peters, A. Sabatini, A. Vacca, *Coord. Chem. Rev.*, 1999, **184,** 311–318.

[29] P. Gans, Protonic Software (2006) "HypSpec" Leeds.

[30] D. H. Amaury, G. Gisèle, P. Christian, G. Serratrice, *Inorg. Chem.,* 2012, **51**, 12142−12151.

[31] G. Serratrice, H. Boukhalfa, C. Beguin, P. Baret, C. Caris, J. L. Pierre, *Inorg. Chem.,1997,* **36,** 3898–3910.

[32] C. Steve, D. Imbert, A. S. Chauvin, G. B. Jean−Claude, *Inorg. Chem.,* 2006, **5**, 732−743.

[33] I. A. Topol, G. J. Tawa, S. K. Burt, A. A. Rashin, *J. Chem. Phys.,* 1999, **111**, 10998–11014.

[34] F. Launay, V. Alain, E. Destandau, N. Ramos, E. Bardez, P. Baret, J. L. Pierre, *New J. Chem.,*2001, **25**, 1269–1280.

[35] G. Kiran, Vaswani, D. K. Mark, *Inorg. Chem.*, 2009, **48**, 5797–5800.

[36] V. Guallar, M. Moreno, J. M. Lluch, F. Amat-Guerri, A. Douhal, *J. Phys. Chem.*, 1996, **100**, 19789–19794.

[37] D. Le Gourrierec, V. A. Kharlanov, R. G. Brown, W. Rettig, *J. Photochem. Photobiol. A.*, 2000, **130**, 101−111.

[38] C. Yuting, W. Hailong, W. Liang, B. Yongzhong, J. Jianzhuang, *J. Org. Chem.,* 2011, **76**, 3774–3781.

[39] Y. Urano, M. Kamiya, T. Kanda, T. Ueno, K. Hirose, T. Nagano, *J. Am. Chem. Soc.*, 2005, **127**, 4888–4894.